CHALMERS

A prestudy of the potential of using finite element analysis for understanding horse accidents

JACOB WASS, KARIN BROLIN

A prestudy of the potential of using finite element analysis for understanding horse accidents

JACOB WASS, KARIN BROLIN

A prestudy of the potential of using finite element analysis for understanding horse accidents

JACOB WASS, KARIN BROLIN

Cover:
THUMS human body model simulating a fall from a horse back on the ground.

Contents

Preface

      October 16, 2015
      Jacob Wass and Karin Brolin

1 OBJECTIVE

This prestudy is an investigation into the potential of using the THUMS [5] model and LS-Dyna [6] simulations to understand the risk of thorax injury in horse related accidents such as horse kicks, tramples, falls from horse backs or rotational falls. A simple model of a security vest was also developed for the THUMS model, to facilitate injury risk comparisons with and without the vest. The severity of thorax injuries was quantified by measuring local stresses and strains in the cortical bone of the ribs, as well as the total deformation of the thorax, measured with Dmax and DcTHOR [2]. This prestudy attempt to answer five questions:

- What is the worst location on the chest to be trampled by a horse with respect to rib fractures?

- How does the stiffness of the ground compound affect the risk of rib fractures when trampled by a horse?

- How does the risk of thorax injuries vary when falling off a horseback in different angles?

- How does the momentum of a horse kick affect the risk of thorax injury on the THUMS model with and without a protective vest?

- How can a rotational fall be modelled and how severe is the injury outcome?

Simulations were set up in LS-Dyna with the THUMS model representing the human body with different environments built up around it representing the scenarios in the five questions. The structure of the report follows the five questions through both the method and results sections.

2   Method

This section describes the simulations performed in the attempt to answer the five questions raised in the Objective. A whole-body Finite Element (FE) Human Body Model (HBM), the Total Human Model for Safety AM50 version 3.0 (Toyota Motor Corporation, Japan) was used, hereafter denoted THUMS. All simulations were performed with the FE solver LS-DYNA (LSTC Inc., Livermore, CA, USA)

The risk of thorax injury was evaluated with stresses and strains measured for each rib, as well as the total deformation of the ribcage. More precisely, the shear stress (τ) and maximum principal strain ($\varepsilon 1$) in the rib cortical bone. The deformation of the ribcage was evaluated with two different measures called Dmax and DcTHOR. Dmax is a maximum relative deformation measure of compression at five points on the ribcage, where 100% means that the thorax was completely compressed at some point and 0% means no compression. DcTHOR is a measure of the maximum deformation between the same points as Dmax, but with emphasis on asymmetric deformation by adding terms measuring the difference of the deformation on the left and right side of the ribcage. Dmax, DcTHOR, τ, and $\varepsilon 1$ was used to measure the risk of obtaining an Abbreviated Injury Scale (AIS) 2+ injury, according to risk curves and a method developed by Mendoza Vázquez et al. [2]. An AIS2+ injury is an injury with two or more rib fractures and/or partial thickness bronchus tear within the soft tissues of the thorax, according to the AIS [10].

MATLAB (The Mathworks Inc., Natick, MA, USA) was used together with LS-PrePost (LSTC Inc, Livermore, CA, USA) to extract the measures needed, with the aid of a developed script, which extracted time history data of shear stress and maximum principal strain from each shell element on the ribs along with the coordinates of six nodes, and saves it as separate files. To calculate the risk of obtaining an AIS2+ injury based on the stress or strain, an algorithm that picked out the maximum element value from the rib with the second highest recorded stress or strain, compared to other ribs, was used. This method ensured that we were evaluating the risk of obtaining two or more rib fractures (AIS2+). The node IDs used for the displacement measures were: mid sternum (D) 89213524, upper left (UL) 89200050, lower left (LL) 89206698, upper right (UR) 89220050, lower right (LR) 89226698 and T9 vertebra (T9) 8913156. The vector between T9 and D was used as a reference of the direction of the thorax. Other vectors were then calculated from the T9 point to the other points and projected on to the unit vector T9 → D, according to Mendoza Vázquez [10]. This method allowed for measuring the deformation of the chest to obtain all points, even though the THUMS model rotated during a simulation.

2.1   Worst chest location to be trampled by a horse

This section describes how estimates were made of the risk of thorax injury from horse hoof impacts to the chest, with initial equal momentum at different locations on the chest, Figure 1. The THUMS model was placed on a rigid plane representing the ground, Figure 2. A gravitational load was applied, along the normal to the ground plane, only to the HBM. The horse hoof was modelled as an oval shaped shell plate with a width of 135 mm and a height of 140 mm in a rigid material. Mass was added with the keyword ELEMENT_MASS_PART which made the full weight of the hoof 125 kg. The hoof model with a mass (m) of 125 kg represents a 500 kg horse putting a fourth of its mass on one hoof with an initial velocity (v_0) directed towards the chest. This resulted in a momentum p = mv_0. The momentum was found by increasing the initial velocity from 0.5 m/s until the risk of sustaining an injury was high, for the case where the chest was trampled in the middle of the sternum (location 6 in Figure 1). The momentum was established at 125 Ns with the 125 kg hoof at a velocity of 1 m/s, since the peak values of shear stress seen in the rib cage was in the range of 60-70 MPa (Figure 3). According to risk curves presented by Mendoza Vázquez [2] this represents a significant risk of injury.

Six different chest locations were tested to evaluate how the risk of fracturing ribs differs as a result of being trampled by a horse, Figure 1. Two of the six locations were located on the sternum, hereafter referred to as low and high. The high point is between the second costal notches and the low between the fourth costal notches. Four more points were added by applying a rotation around the spine, Figure 1. The legs were not included in the simulation since they were considered to have little or no influence on the results of interest.

(a)   (b)
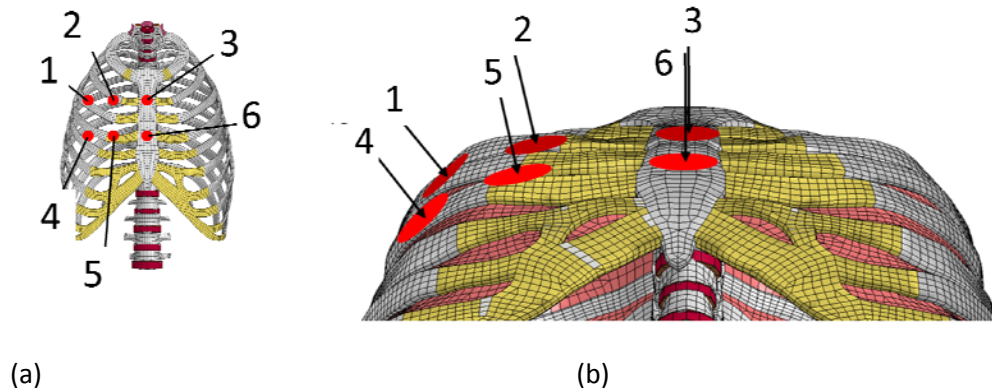
Figure 1: Tested locations on the THUMS chest illustrated with red circles: (a) from a front view, and (b) from a bottom view with arrows to show the angle of the trample.

Figure 2: Model of THUMS being trampled by a horse hoof. 1: horse hoof, 2: THUMS, and 3: rigid wall representing the ground.

Figure 3: Shear stress in the THUMS cortical bone as a result of being trampled by a horse hoof (125Ns) at 0, 20, 50 and 80 ms. Shear stress higher than 60 MPa is displayed in red which indicate that the risk of sustaining an AIS2+ injury is higher than 50% [2].

2.2 INFLUENCE OF GROUND STIFFNESS ON INJURY RISK

Two simulations were set up modelling a person lying on the ground being trampled by a horse hoof, see Figure 4. A gravitational load was applied to the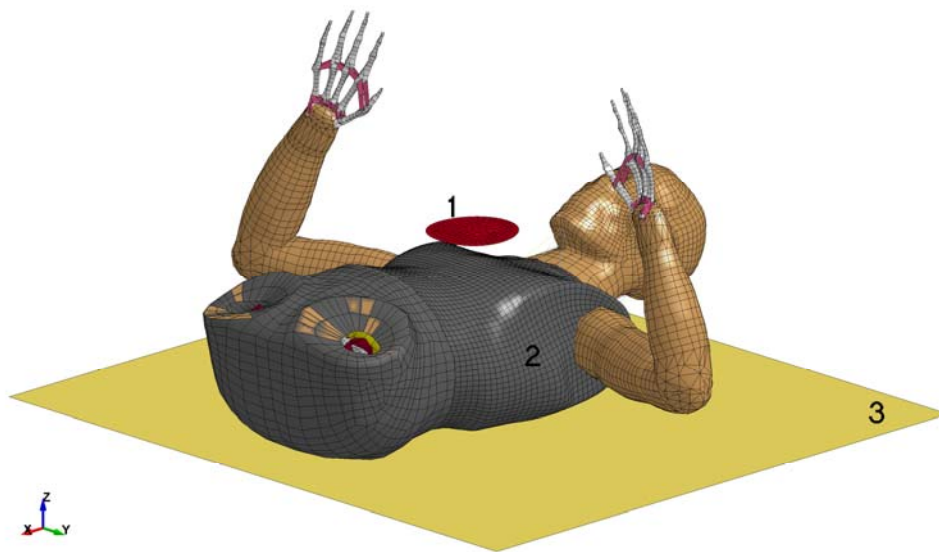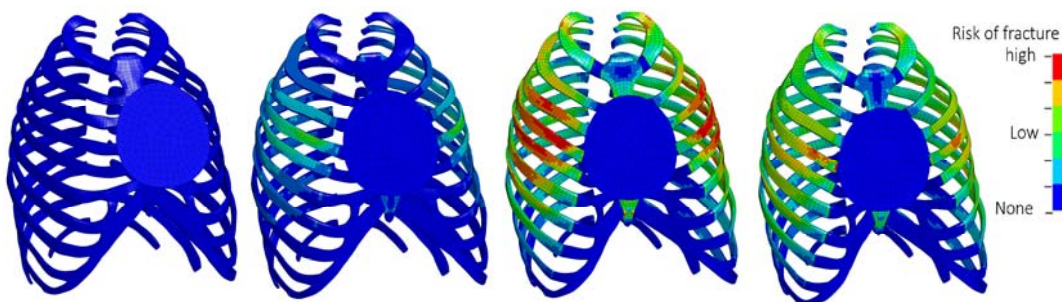 THUMS model, but not the hoof. The weight of the hoof was 125 kg and the initial velocity was set to 1 m/s, as described in section 2.1.

The stiffness of the ground material was modelled as two different extremes. One of the ground materials was modelled as soft clay and the other one as dense dry sand. The LS-Dyna material type MAT_SOIL_AND_FOAM was used due to its simplicity and property of pressure dependent stiffness. The density, bulk and shear modulus were taken from a technical report on computer material models for soils [4], whereas the pressure dependency and yield behaviour were derived from an article about soft soil impact [3], see Table I. The material has the ability to flow. Therefore, a boundary condition prevents the ground material from moving in the XYZ -direction along all surfaces except the top surface, which is free. The ground was modelled as a solid block of hexahedral finite elements, with null shells on the top surface to improve the contact interaction.

TABLE I
Ground material properties used with MAT_SOIL_AND_FOAM.

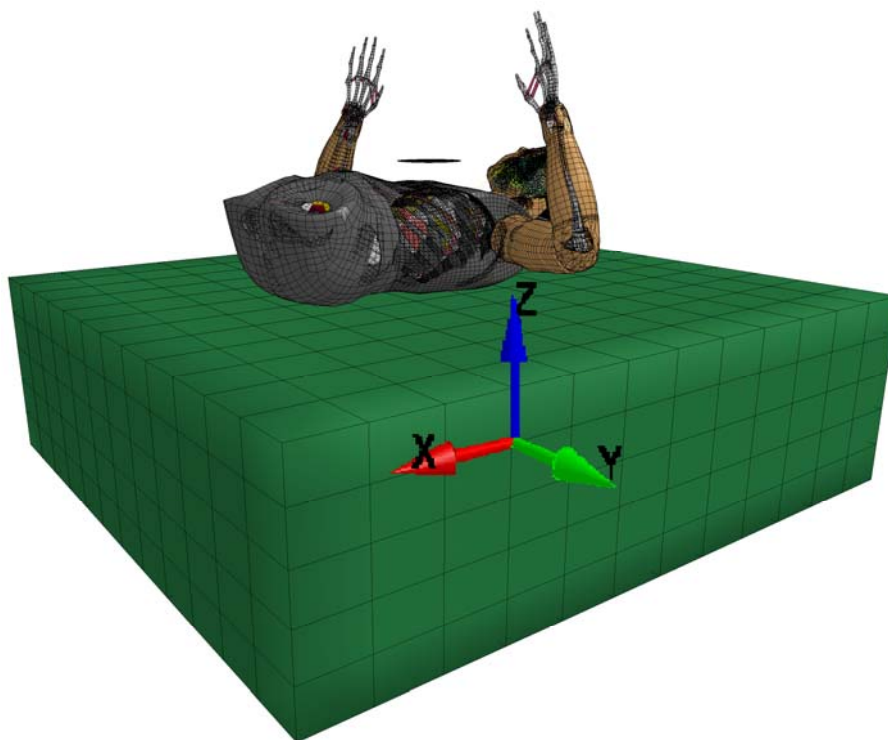| Ground material	Density [kg/mm3]	Bulk modulus [GPa]	Shear modulus [Gpa]	a0	a1	a2
Soft clay	1.36e-6	1.4e-3	1.00e-3	0	0	0.3
Dense dry sand	1.82e-6	68.7e-3	18.8e-3	0	0	0.3

Figure 4: Model to simulate horse trample and the effect of ground material.

2.3 THORAX INJURIES SUSTAINED WHEN FALLING FROM THE BACK OF A HORSE

Simulations were set up modelling a person falling from 1.5 meters, resulting in a vertical velocity (v) at impact of 5.4 m/s (v = √2gh = 5.4 m/s). A horizontal velocity of 15 km/h was also included to simulate a fall from a moving horse. The reference initial position can be seen in Figure 5a. Then, from this positions two rotations were performed around the x-axis (Figures 5 b and c) and two combinations of x and y-rotations (Figures 5 d and e). The global coordinate system referred to herein originates between the centres of the hip joints in the reference model and was oriented as the coordinate system in Figure 4. The legs of the THUMS model were added to include inertial effects and to achieve more visually appealing results.

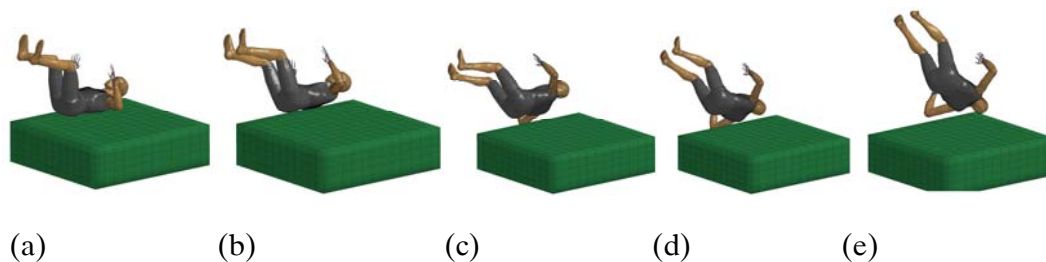| (a) | (b) | (c) | (d) | (e) |

Figure 5: Five different fall scenarios: a) reference position, b) 25 degrees X-rotation, c) 50 degrees X-rotation, d) 50 degrees X rotation and -20 degrees Y-rotation, and e) 50 degrees X rotation and -40 degrees Y-rotation. Coordinate system defined in Figure 4.

2.4 VARIATION OF THE MOMENTUM OF A HORSE KICK

The THUMS model was positioned vertically without ground contact. The horse hoof was directed towards the chest, location 6 in Figure 1 according to section 2.1. Gravity was not included in the simulation. The momentum of the hoof was varied such that the mass was constant at 125 kg and the velocity changed from 0.6 m/s up to 4.0 m/s. This gave an investigated momentum range from 75 - 500 Ns. This range was investigated with steps of 25 Ns, resulting in 18 simulations.

2.5 ROTATIONAL FALL AND INJURY OUTCOME

A rotational fall is a serious type of accident caused by a horse stumbling on an obstacle and falling with a rotating motion down behind the obstacle. Occasionally, the rider is squashed under the horse, with serious or fatal injuries as the outcome. To construct this event in a simulation, a simple model of a horse was built by reconstructing the outer shape of a horse seen from the side with splines in the software CATIA version 5 (3DS Dassault Systèmes, Paris, France). An oval section was swept along the profile, followed by scaling of the geometry so that the weight of the horse increased to 500 kg, at a density of 1e-6 kg/mm. The geometry was meshed in the software Hypermesh (Altair Engineering, Troy, MI, USA), with an automatic tetrahedon mesher. The average element size was set to 30 mm. The material of the horse model was copied from the bulk material in the THUMS leg flesh. This is a viscoelastic material (MAT_VISCOELASTIC), with a bulk module of 2.356e-3 GPa, a short time shear modulus of 3.406e-4 GPa, a long time shear modulus of 1.17e-4 GPa and a decay constant of 0.1. The initial velocity and rotational velocity was estimated by assuming a riding velocity of 30 km/h and that the horse hits a rigid obstacle at a point 50 cm away from its centre of gravity. Then 70% of the translational kinetic energy was assumed to change to rotational kinetic energy and to translational energy in the riding direction. The rotational inertia of the horse around its centre of gravity was measured with LS-PrePost to $0.16e9$ kgmm^2. With these assumptions, the rotational velocity became 6 rad/s and was calculated from $mv^2 = 0.70(I_{CoG} + mr^2)\omega^2$, where r is the distance from the centre of gravity of the horse to the obstacle. The translational velocity that accounted for 30% of the energy was calculated to 5 m/s. Initial velocity was initiated in the simulation with the keyword

INITIAL_VELOCITY_GENERATION, in which instantaneous centre (in this case the obstacle), rotation and translational velocities were specified. The THUMS model was placed to represent a rider doing a front flip and landing back first on the ground. The impact of the horse was at the chest/stomach of the rider. The ground was modelled as dense sand with the properties in Table I.

2.6 CREATION OF A SECURITY VEST

A simplified version of a security vest, typical of those worn by horse riders [9], was created by covering the inside and outside of a solid foam core in a nylon fabric. The THUMS model was imported to the Hypermesh software, exporting the torso surfaces as an IGES geometry file into CATIA V5. The outer edges of the vest were created by inserting splines through points placed at the surface geometry from the imported THUMS surfaces. When the outer edges were done, some supporting splines were added, attached along the THUMS geometry which allowed creation of the vest surface by two functions called multi-section surface and fill.

Next the vest geometry was imported to Hypermesh as an IGES geometry file, and then meshed using a surface meshing tool with mixed quad and triangular elements of 15 mm in average size. LS-PrePost was used to create two layers of solid hexahedral elements as a 20 mm offset from the inner surface. Finally, an outer surface was created on top of the solid surface. All coincident nodes were merged, representing the inner and outer fabrics being tightly glued to the foam core. The nylon material was modelled with a shell thickness of 0.5 mm and the LS-Dyna material MAT_ELASTIC. Material data for the nylon was derived from an online database called MatWeb [8]. The foam material was modelled with the material MAT_LOW_DENSITY_FOAM, and its data was taken from an example available online [8]. Material data can be found in Table 2. A picture of the final vest model can be seen in Figure 7.

TABLE II
Security vest material properties

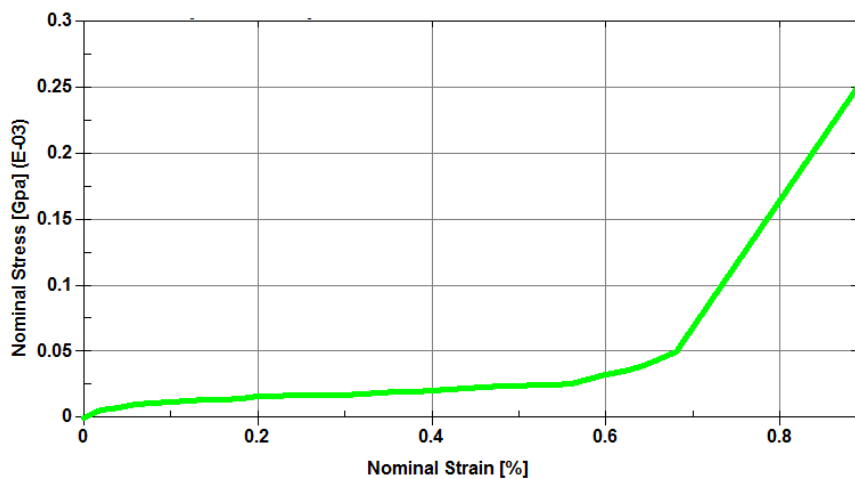| Material	Type [7]	Density [kg/mm³]	Young's modulus [GPa]	Poison's ratio [%]	Stress-strain relation	Ref
Nylon fabric	MAT_001	1.00e-6	2.00	0.32	Linear	[8]
Foam core	MAT_005	2.40e-7	-	-	Figure 6	[1]

Figure 6: Nominal stress versus strain curve used to model the foam material in the core of the security vest.
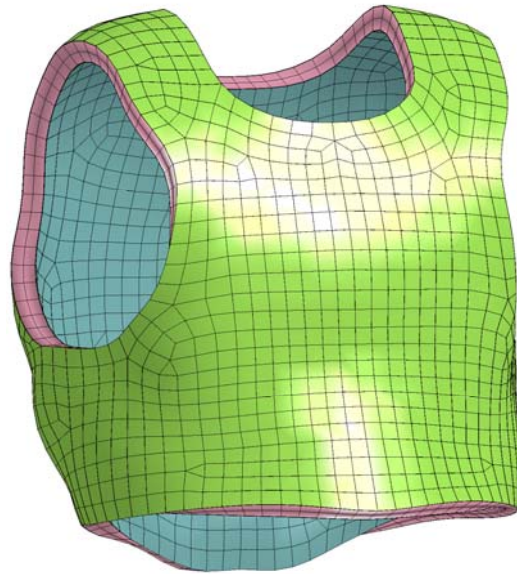
Figure 7: Nominal stress versus strain curve used to model the foam material in the core of the security vest.

3 RESULTS

3.1 WORST CHEST LOCATION TO BE TRAMPLED BY A HORSE

In the simulations conducted without a security vest when being trampled at a momentum of 125 Ns, two of the six tested trample locations on the chest resulted in a 100% risk of sustaining an AIS2+ injury (Table III). The two locations were the low central location 6 and the low angled location 5. The measure that indicated a high risk of injury in the low central location 6 was the shear stress in the cortical bone of the ribs, while in the slightly angled location 5 it was the differential deflection criterion DcTHOR that indicated the highest risk of injury. Shear stresses above 60 MPa could be seen at the sternum and on the 3rd, 4th and 5th ribs during both the central and angled low simulations. The other tests did not indicate as high as 100% risk of sustaining an AIS2+ injury, however the risks were still high for location 4 (91%), 3 (87%) and 2 (82%). With the security vest worn by the THUMS, no injury was predicted for any of the tested locations. The highest risk with the vest was seen in the high central location 3 (25%) and high angled location 2 (11%).

3.2 INFLUENCE OF GROUND STIFFNESS ON INJURY RISK

It was possible to observe the influence of the ground stiffness on the injury risk. When the THUMS model was trampled on dense sand a similar injury risk was observed, as on completely rigid ground (Table IV). The shear stress in the 4th ribs was above the failure threshold. Also the AIS2+ risk was predicted to 100% for the shear stress. However, when the rider was trampled on a soft clay material it was observed that the risk of sustaining an AIS2+ injury was reduced by more than half and no ribs were predicted to fracture. As expected, the benefit when wearing a security vest is obvious even when ground stiffness has been taken into account. Very low AIS2+ injury risks were estimated with the vested models on both grounds.

3.3 THORAX INJURIES SUSTAINED WHEN FALLING FROM THE BACK OF A HORSE

Rib fractures and high risk of AIS2+ injuries were estimated in all of the five fall simulations that were conducted (Table V). An observed trend was that in the simulations where THUMS was falling with its head first tended to cause more fractured ribs (6-7 fractured ribs) compared to the more flat landings where the thorax posture was perpendicular to the ground (2-4 fractured ribs). In the simulations with the head first, the THUMS rotated around the Y-axis while the flat landings produced X-rotation only. The predicted risk of AIS 2+ injury was 100 % for all fall simulations, with the maximum shear stress reaching values of 69 - 121 MPa.

3.4 VARIATION OF THE MOMENTUM OF A HORSE KICK

The AIS2+ risk of injury versus the kick momentum is plotted in Figure 8. Without a vest, simulations suggest that the risk of injury quickly begin to increase if the kick momentum is higher than 225 Ns. In addition to that, the Dmax measure estimated a risk of 0–10% if the kick momentum is as low as 100 Ns. The security vest had a clear effect on the risk of injury since it offsets the level of momentum that the chest can withstand with approximately 125-175 Ns.

Comparing the risk functions, the most conservative, in terms of risk prediction, was shear stress (τ), followed by the chest compression measure (Dmax), maximum principal strain (ε), and finally the differential deflection measure (DcTHOR).

TABLE III
AIS2+ INJURY RISK FOR DIFFERENT TRAMPLE LOCATIONS

The maximum predicted AIS2+ risk estimated using shear stress (τ), maximum principle strain (ε_1), differential chest deflection (DcTHOR), and relative chest compression (Dmax). Images show the deformed ribcage with a contour plot of the average shear stress in each element, red colour indicates $\tau > 60$ MPa and dark blue $\tau = 0$ MPa. Predicted rib fracture location (BR) is indicated for left (L) and right (R) side with rib number.
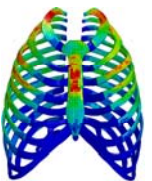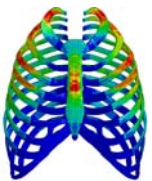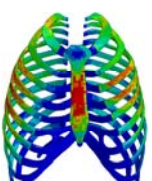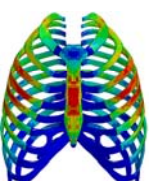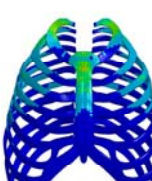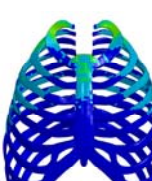
Location 1	Location 2	Location 3
$\tau = 0\%$	$\tau = 20\%$	$\tau = 78\%$
$\varepsilon_1 = 8\%$	$\varepsilon_1 = 82\%$	$\varepsilon_1 = 87\%$
DcTHOR= 1%	DcTHOR= 30%	DcTHOR= 1%
Dmax = 53%	Dmax = 61%	Dmax = 74%
BR: -	BR: R1	BR: L1 R1

Location 4	Location 5	Location 6
$\tau = 80\%$	$\tau = 1\%$	$\tau = 100\%$
$\varepsilon_1 = 39\%$	$\varepsilon_1 = 23\%$	$\varepsilon_1 = 55\%$
DcTHOR= 22%	DcTHOR= 100%	DcTHOR= 26%
Dmax = 91%	Dmax = 84%	Dmax = 84%
BR: R6	BR: -	BR: L4 R4

Location 1 with vest	Location 2 with vest	Location 3 with vest
$\tau = 0\%$	$\tau = 0\%$	$\tau = 0\%$
$\varepsilon_1 = 0\%$	$\varepsilon_1 = 11\%$	$\varepsilon_1 = 25\%$
DcTHOR= 0%	DcTHOR= 0%	DcTHOR= 0%
Dmax = 0%	Dmax = 1%	Dmax = 11%
BR: -	BR: -	BR: -

Location 4 with vest	Location 5 with vest	Location 6 with vest
$\tau = 0\%$	$\tau = 0\%$	$\tau = 0\%$
$\varepsilon_1 = 0\%$	$\varepsilon_1 = 0\%$	$\varepsilon_1 = 0\%$
DcTHOR= 0%	DcTHOR= 0%	DcTHOR= 0%
Dmax = 1%	Dmax = 5%	Dmax = 4%
BR: -	BR: -	BR: -

TABLE IV
EFFECT GROUND HAS ON AIS2+ INJURY RISK

The maximum predicted AIS2+ risk estimated from simulations when trampled on different ground materials using shear stress (τ), maximum principle strain (ε), differential chest deflection (DcTHOR), and relative chest compression (Dmax). Predicted rib fracture location (BR) is indicated for left (L) and right (R) side with rib number. The images illustrate the ground and chest deformation when chest compression was at its peak value.

Dense sand

Soft clay
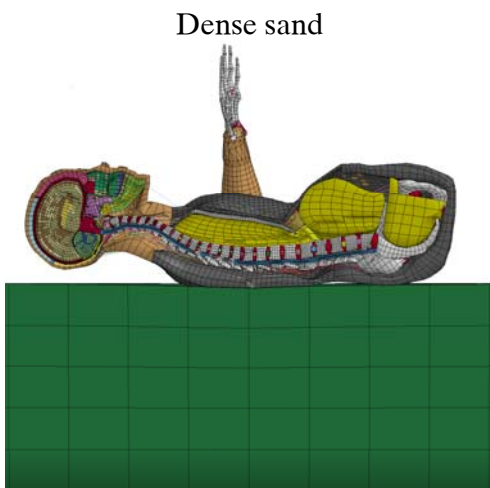
$\tau = 100\%$
$\varepsilon_1 = 56\%$
DcTHOR = 10%
Dmax = 76%
BR: L4 R4

$\tau = 40\%$
$\varepsilon_1 = 18\%$
DcTHOR = 0%
Dmax = 15%
BR: -

Dense sand with vest

Soft clay with vest
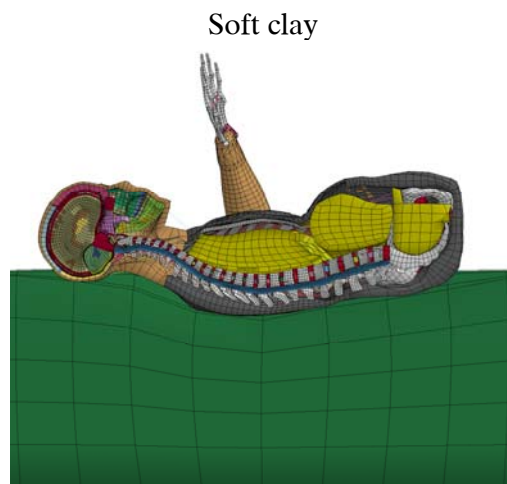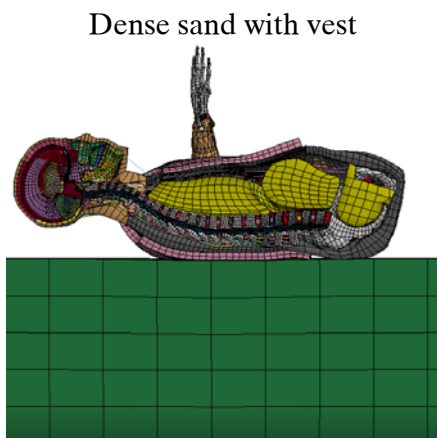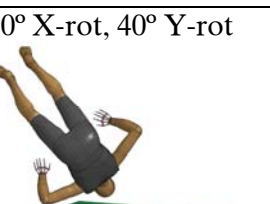
$\tau = 0\%$
$\varepsilon_1 = 0\%$
DcTHOR = 0%
Dmax = 3%
Broken ribs: -
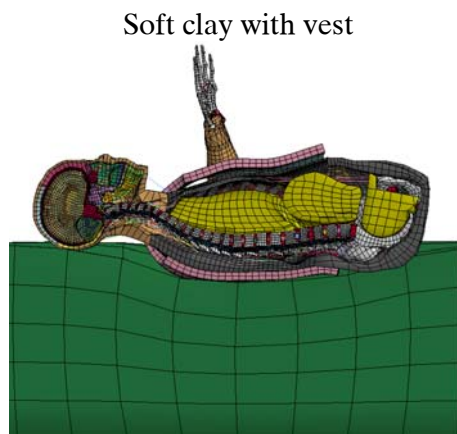
$\tau = 0\%$
$\varepsilon_1 = 0\%$
DcTHOR = 0%
Dmax = 0%
Broken ribs: -

TABLE V
FALL AIS2+ INJURY RISK

The maximum predicted AIS2+ risk estimated from fall simulations using shear stress (τ), maximum principle strain (ε), differential chest deflection (DcTHOR), and relative chest compression (Dmax). Predicted rib fracture location (BR) is indicated for left (L) and right (R) side with rib number. The images illustrate a sequence of three points in time (t) during the fall simulations.

t_{start}	t_{mid}	t_{end}	AIS2+ risk
Reference angle			
			$\tau = 99\%$
			$\varepsilon1 = 55\%$
			DcTHOR=100%
			Dmax = 85%
			BR: R4 R7
25° X-rot			
			$\tau = 100\%$
			$\varepsilon1 = 82\%$
			DcTHOR=100%
			Dmax = 85%
			BR: L7 R1 R7 R8
50° X-rot			
			$\tau = 100\%$
			$\varepsilon1 = 99\%$
			DcTHOR=100%
			Dmax = 61%
			BR: R1 R7 R8
50° X-rot, 20° Y-rot			
			$\tau = 100\%$
			$\varepsilon1 = 100\%$
			DcTHOR=100%
			Dmax = 43%
			BR: R1 R2 R4 R6 R7 R8 R9
50° X-rot, 40° Y-rot			
			$\tau = 100\%$
			$\varepsilon1 = 92\%$
			DcTHOR=100%
			Dmax = 7%
			BR: L1 R1 R4 R6 R7 R8
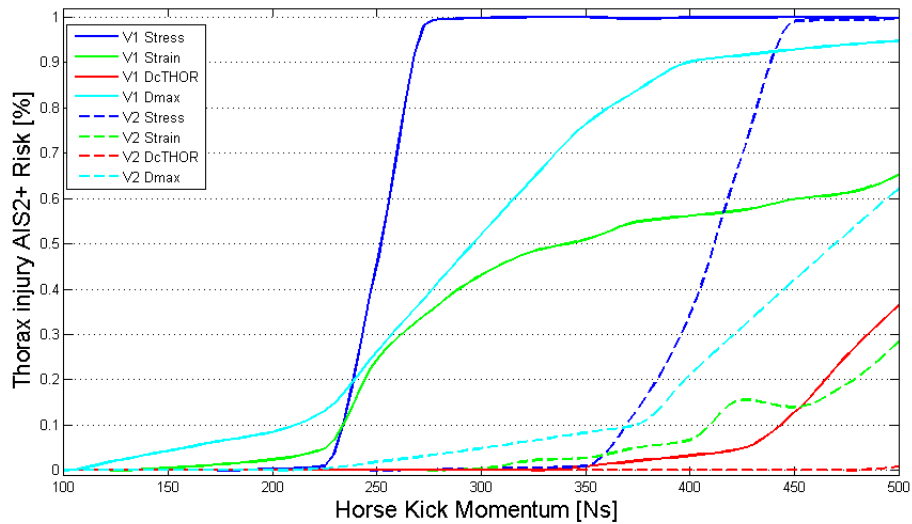
Figure 8: Results of thorax AIS2+ injury risk versus horse kick momentum.

3.5   ROTATIONAL FALL AND INJURY OUTCOME

It was possible to simulate the rotational fall until a few tenths of a millisecond into the impact between the horse and rider. After that, the simulation crashed due to negative volumes in finite elements. Negligible differences in injury risk was seen between the vested and non-vested models, since both of them estimated 100% risk of sustaining an AIS2+ injury on all measures. All ribs from one to nine also showed shear stress values above 65 MPa, which indicates that they would break. The compression of the ribcage was 49% for the non-vested and 51% for the vested THUMS. See Figure 9 for a picture of the end of the simulation and plots of the shear stress in the ribs.
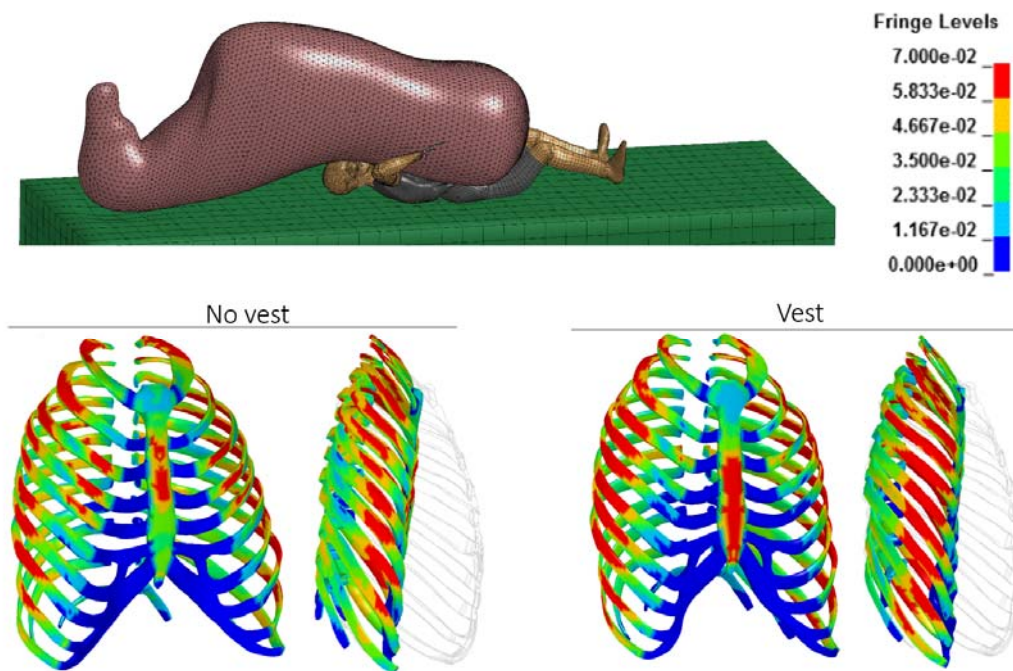
Figure 9: Illustration of the end state of the rotational fall simulation (top), and with a contour plot of the average shear stress (red colour indicates τ > 60 MPa and dark blue τ = 0 MPa) in the rib cage for both the vested and non-vested THUMS including a light grey contour indicating the initial rib cage geometry.

4 REFERENCES

[1] Dynaexamples.com/sph/foam. Ls-dyna examples of foam material modelling, August 2015.

[2] Mendoza Vázquez M, et. al. Evaluation of thoracic injury criteria for THUMS finite element human body model using real-world crash data. Volume IRC-14-62. IRCOBI Conference, 2014.

[3] Fasanella and Jacksson et al. Soft soil impact testing and simulation of aerospace structures. In 10th international LS-Dyna Users Conference, 2008.

[4] Harris and David W. Computer material models for soils using flac and dyna. U.S. Department of the Interior, Bureau of Reclamation, 2006.

[5] Iwamoto M, Kisanuki Y, Watanabe I, Furusu K, and Miki K. Development of a finite element model of the total human model for safety (thums) and application to injury reconstruction, 2002.

[6] Livermore Software Technology Corporation. LS-Dyna Theory Manual, 2006.

[7] Livermore Software Technology Corporation. LS-Dyna Keyword User's Manual Volume 2, Material Models, 2012.

[8] MatWeb.com. Material property data for nylon 6, unreinforced, August 2015.

[9] Smartpakequine. www.smartpakequine.com/protective-vests-and-safety-824pc, August 2015.

[10] Mendoza Vázquez M. Thoracic injury in frontal car crashes: risk assessment using a finite element human body model. 2014.

5 APPENDIX

TABLE VI: LIST OF SIMULATIONS

Section	Load case	Security Vest	Ground**	Mass [kg]	Impactor Velocity [m/s]	Impactor Location *	Fall Angle [deg] X-rot	Fall Angle [deg] Y-rot	File name [VEST_SimID_explaination]
2.1	Hoof trample	no	Rigid wall	125	1.00	6	-	-	V1_1_Trampled_angle_0_variation_stiff_ground
2.1	Hoof trample	no	Rigid wall	125	1.00	5	-	-	V1_2_Trampled_angle_20_variation_stiff_ground
2.1	Hoof trample	no	Rigid wall	125	1.00	4	-	-	V1_3_Trampled_angle_40_variation_stiff_ground
2.1	Hoof trample	no	Rigid wall	125	1.00	3	-	-	V1_4_Trampled_angle_0H_variation_stiff_ground
2.1	Hoof trample	no	Rigid wall	125	1.00	2	-	-	V1_5_Trampled_angle_20H_variation_stiff_ground
2.1	Hoof trample	no	Rigid wall	125	1.00	1	-	-	V1_6_Trampled_angle_40H_variation_stiff_ground
2.2	Hoof trample	no	Soft Clay	125	1.00	6	-	-	V1_7_Trampled_angle_0_variation_Soft_sand
2.2	Hoof trample	no	Dense Sand	125	1.00	6	-	-	V1_8_Trampled_angle_0_variation_Dense_sand
2.3	Fall	no	Dense Sand	-	-	-	0	0	V1_9_Fall_angle_1xy_variation_Dense_sand
2.3	Fall	no	Dense Sand	-	-	-	25	0	V1_10_Fall_angle_2x_variation_Dense_sand
2.3	Fall	no	Dense Sand	-	-	-	50	0	V1_11_Fall_angle_3x_variation_Dense_sand
2.3	Fall	no	Dense Sand	-	-	-	50	20	V1_12_Fall_angle_2xy_variation_Dense_sand
2.3	Fall	no	Dense Sand	-	-	-	50	40	V1_13_Fall_angle_3xy_variation_Dense_sand
2.4	Horse kick	no	none	125	0.6	6	-	-	V1_3_impuls_0_6_vs_fracture_risk_horse_kick
2.4	Horse kick	no	none	125	0.8	6	-	-	V1_4_impuls_0_8_vs_fracture_risk_horse_kick
2.4	Horse kick	no	none	125	1.0	6	-	-	V1_5_impuls_1_0_vs_fracture_risk_horse_kick
2.4	Horse kick	no	none	125	1.2	6	-	-	V1_6_impuls_1_2_vs_fracture_risk_horse_kick
2.4	Horse kick	no	none	125	1.4	6	-	-	V1_7_impuls_1_4_vs_fracture_risk_horse_kick
2.4	Horse kick	no	none	125	1.6	6	-	-	V1_8_impuls_1_6_vs_fracture_risk_horse_kick
2.4	Horse kick	no	none	125	1.8	6	-	-	V1_9_impuls_1_8_vs_fracture_risk_horse_kick
2.4	Horse kick	no	none	125	2.0	6	-	-	V1_10_impuls_2_0_vs_fracture_risk_horse_kick
2.4	Horse kick	no	none	125	2.2	6	-	-	V1_11_impuls_2_2_vs_fracture_risk_horse_kick
2.4	Horse kick	no	none	125	2.4	6	-	-	V1_12_impuls_2_4_vs_fracture_risk_horse_kick
2.4	Horse kick	no	none	125	2.6	6	-	-	V1_13_impuls_2_6_vs_fracture_risk_horse_kick
2.4	Horse kick	no	none	125	2.8	6	-	-	V1_14_impuls_2_8_vs_fracture_risk_horse_kick
2.4	Horse kick	no	none	125	3.0	6	-	-	V1_15_impuls_3_0_vs_fracture_risk_horse_kick
2.4	Horse kick	no	none	125	3.2	6	-	-	V1_16_impuls_3_2_vs_fracture_risk_horse_kick
2.4	Horse kick	no	none	125	3.4	6	-	-	V1_17_impuls_3_4_vs_fracture_risk_horse_kick
2.4	Horse kick	no	none	125	3.6	6	-	-	V1_18_impuls_3_6_vs_fracture_risk_horse_kick
2.4	Horse kick	no	none	125	3.8	6	-	-	V1_19_impuls_3_8_vs_fracture_risk_horse_kick
2.4	Horse kick	no	none	125	4.0	6	-	-	V1_20_impuls_4_0_vs_fracture_risk_horse_kick
2.5	Rotational fall	no	Dense Sand	500	***	-	0	-55	V1_14_Rotational_fall_Dense_sand
2.1	Hoof trample	yes	Rigid wall	125	1.00	6	-	-	V2_1_Trampled_angle_0_variation_stiff_ground
2.1	Hoof trample	yes	Rigid wall	125	1.00	5	-	-	V2_2_Trampled_angle_20_variation_stiff_ground
2.1	Hoof trample	yes	Rigid wall	125	1.00	4	-	-	V2_3_Trampled_angle_40_variation_stiff_ground
2.1	Hoof trample	yes	Rigid wall	125	1.00	3	-	-	V2_4_Trampled_angle_0H_variation_stiff_ground
2.1	Hoof trample	yes	Rigid wall	125	1.00	2	-	-	V2_5_Trampled_angle_20H_variation_stiff_ground
2.1	Hoof trample	yes	Rigid wall	125	1.00	1	-	-	V2_6_Trampled_angle_40H_variation_stiff_ground
2.2	Hoof trample	yes	Soft Clay	125	1.00	6	-	-	V2_7_Trampled_angle_0_variation_Soft_sand
2.2	Hoof trample	yes	Dense Sand	125	1.00	6	-	-	V2_8_Trampled_angle_0_variation_Dense_sand
2.3	Fall	yes	Dense Sand	-	-	-	0	0	V2_9_Fall_angle_1xy_variation_Dense_sand
2.3	Fall	yes	Dense Sand	-	-	-	25	0	V2_10_Fall_angle_2x_variation_Dense_sand
2.3	Fall	yes	Dense Sand	-	-	-	50	0	V2_11_Fall_angle_3x_variation_Dense_sand
2.3	Fall	yes	Dense Sand	-	-	-	50	20	V2_12_Fall_angle_2xy_variation_Dense_sand
2.3	Fall	yes	Dense Sand	-	-	-	50	40	V2_13_Fall_angle_3xy_variation_Dense_sand
2.4	Horse kick	yes	none	125	0.6	6	-	-	V2_3_impuls_0_6_vs_fracture_risk_horse_kick
2.4	Horse kick	yes	none	125	0.8	6	-	-	V2_4_impuls_0_8_vs_fracture_risk_horse_kick
2.4	Horse kick	yes	none	125	1.0	6	-	-	V2_5_impuls_1_0_vs_fracture_risk_horse_kick
2.4	Horse kick	yes	none	125	1.2	6	-	-	V2_6_impuls_1_2_vs_fracture_risk_horse_kick
2.4	Horse kick	yes	none	125	1.4	6	-	-	V2_7_impuls_1_4_vs_fracture_risk_horse_kick
2.4	Horse kick	yes	none	125	1.6	6	-	-	V2_8_impuls_1_6_vs_fracture_risk_horse_kick
2.4	Horse kick	yes	none	125	1.8	6	-	-	V2_9_impuls_1_8_vs_fracture_risk_horse_kick
2.4	Horse kick	yes	none	125	2.0	6	-	-	V2_10_impuls_2_0_vs_fracture_risk_horse_kick
2.4	Horse kick	yes	none	125	2.2	6	-	-	V2_11_impuls_2_2_vs_fracture_risk_horse_kick
2.4	Horse kick	yes	none	125	2.4	6	-	-	V2_12_impuls_2_4_vs_fracture_risk_horse_kick
2.4	Horse kick	yes	none	125	2.6	6	-	-	V2_13_impuls_2_6_vs_fracture_risk_horse_kick
2.4	Horse kick	yes	none	125	2.8	6	-	-	V2_14_impuls_2_8_vs_fracture_risk_horse_kick
2.4	Horse kick	yes	none	125	3.0	6	-	-	V2_15_impuls_3_0_vs_fracture_risk_horse_kick
2.4	Horse kick	yes	none	125	3.2	6	-	-	V2_16_impuls_3_2_vs_fracture_risk_horse_kick
2.4	Horse kick	yes	none	125	3.4	6	-	-	V2_17_impuls_3_4_vs_fracture_risk_horse_kick
2.4	Horse kick	yes	none	125	3.6	6	-	-	V2_18_impuls_3_6_vs_fracture_risk_horse_kick
2.4	Horse kick	yes	none	125	3.8	6	-	-	V2_19_impuls_3_8_vs_fracture_risk_horse_kick
2.4	Horse kick	yes	none	125	4.0	6	-	-	V2_20_impuls_4_0_vs_fracture_risk_horse_kick
2.5	Rotational fall	yes	Dense Sand	500	***	-	0	-55	V2_14_Rotational_fall_Dense_sand

*See Figure 3 for more info about the locations
**See subsection 2.2 for more info about the ground materials
*** The entire horse has an initial velocity and rotation, see subsection 2.5

The maximum estimated shear stress (τ), maximum principle strain (ε), differential chest deflection (DcTHOR), and relative chest compression (Dmax) for all simulations. The last four columns provide results normalised with the trample simulation at the lower sternum location 6.

File Name	τ	ε_1	DcTHOR	Dmax	Nshear	Nstrain	NDcTHOR	Ndmax
[VEST_SimID_explaination]	[MPa]	[%]	[mm]	[%]	[%]	[%]	[%]	[%]
V1_1_Trampled_angle_0_variation_stiff_ground	74.56	2.66	44.70	32.36	100	100	100	100
V1_2_Trampled_angle_20_variation_stiff_ground	64.64	1.54	72.72	32.36	87	58	163	100
V1_3_Trampled_angle_40_variation_stiff_ground	66.08	2.10	43.88	34.70	89	79	98	107
V1_4_Trampled_angle_0H_variation_stiff_ground	64.82	3.78	31.74	29.88	87	142	71	92
V1_5_Trampled_angle_20H_variation_stiff_ground	65.48	4.30	45.53	27.74	88	162	102	86
V1_6_Trampled_angle_40H_variation_stiff_ground	56.18	1.79	31.61	26.62	75	67	71	82
V1_7_Trampled_angle_0_variation_Soft_sand	63.49	1.35	24.39	20.77	85	51	55	64
V1_8_Trampled_angle_0_variation_Dense_sand	72.93	3.16	41.01	30.21	98	119	92	93
V1_9_Fall_angle_1xy_variation_Dense_sand	69.90	2.53	160.02	32.54	94	95	358	101
V1_10_Fall_angle_2x_variation_Dense_sand	80.69	3.49	174.14	32.62	108	131	390	101
V1_11_Fall_angle_3x_variation_Dense_sand	85.17	7.20	235.78	27.83	114	271	527	86
V1_12_Fall_angle_2xy_variation_Dense_sand	121.57	24.15	149.11	24.95	163	908	334	77
V1_13_Fall_angle_3xy_variation_Dense_sand	100.35	14.28	116.36	16.54	135	537	260	51
V1_3_impuls_0_6_vs_fracture_risk_horse_kick	28.60	0.29	8.79	7.75	38	11	20	24
V1_4_impuls_0_8_vs_fracture_risk_horse_kick	37.50	0.38	11.32	9.95	50	14	25	31
V1_5_impuls_1_0_vs_fracture_risk_horse_kick	46.22	0.47	13.66	12.13	62	18	31	37
V1_6_impuls_1_2_vs_fracture_risk_horse_kick	51.78	0.56	15.84	14.30	69	21	35	44
V1_7_impuls_1_4_vs_fracture_risk_horse_kick	54.09	0.66	18.24	16.44	73	25	41	51
V1_8_impuls_1_6_vs_fracture_risk_horse_kick	56.59	0.83	20.25	18.48	76	31	45	57
V1_9_impuls_1_8_vs_fracture_risk_horse_kick	59.70	1.07	22.07	20.48	80	40	49	63
V1_10_impuls_2_0_vs_fracture_risk_horse_kick	63.74	1.53	24.05	22.46	85	57	54	69
V1_11_impuls_2_2_vs_fracture_risk_horse_kick	67.37	1.81	25.95	24.42	90	68	58	75
V1_12_impuls_2_4_vs_fracture_risk_horse_kick	69.49	2.03	27.92	26.41	93	76	62	82
V1_13_impuls_2_6_vs_fracture_risk_horse_kick	70.32	2.16	29.87	28.36	94	81	67	88
V1_14_impuls_2_8_vs_fracture_risk_horse_kick	70.08	2.22	31.76	30.36	94	84	71	94
V1_15_impuls_3_0_vs_fracture_risk_horse_kick	69.37	2.32	34.21	32.38	93	87	77	100
V1_16_impuls_3_2_vs_fracture_risk_horse_kick	70.35	2.39	36.46	34.24	94	90	82	106
V1_17_impuls_3_4_vs_fracture_risk_horse_kick	70.18	2.40	39.54	35.90	94	90	88	111
V1_18_impuls_3_6_vs_fracture_risk_horse_kick	70.36	2.48	41.70	37.42	94	93	93	116
V1_19_impuls_3_8_vs_fracture_risk_horse_kick	69.96	2.53	44.49	38.71	94	95	100	120
V1_20_impuls_4_0_vs_fracture_risk_horse_kick	69.39	2.67	46.97	39.65	93	100	105	123
V1_14_Rotational_fall_Dense_sand	84.86	6.79	103.33	51.22	114	255	231	158
V2_1_Trampled_angle_0_variation_stiff_ground	35.86	0.47	16.41	13.50	48	18	37	42
V2_2_Trampled_angle_20_variation_stiff_ground	37.36	0.56	15.57	14.70	50	21	35	45
V2_3_Trampled_angle_40_variation_stiff_ground	37.08	0.41	16.73	11.09	50	16	37	34
V2_4_Trampled_angle_0H_variation_stiff_ground	48.80	1.57	11.08	10.72	65	59	25	33
V2_5_Trampled_angle_20H_variation_stiff_ground	47.17	1.32	11.71	11.15	63	50	26	34
V2_6_Trampled_angle_40H_variation_stiff_ground	30.72	0.25	10.95	7.27	41	9	24	22
V2_7_Trampled_angle_0_variation_Soft_sand	29.28	0.22	8.35	5.49	39	8	19	17
V2_8_Trampled_angle_0_variation_Dense_sand	44.31	0.53	20.97	12.94	59	20	47	40
V2_9_Fall_angle_1xy_variation_Dense_sand	70.34	2.36	119.56	32.31	94	89	267	100
V2_10_Fall_angle_2x_variation_Dense_sand	60.83	2.68	123.98	23.48	82	101	277	73
V2_11_Fall_angle_3x_variation_Dense_sand	81.98	9.95	123.22	21.14	110	374	276	65
V2_12_Fall_angle_2xy_variation_Dense_sand	110.33	20.12	27.84	15.62	148	756	62	48
V2_13_Fall_angle_3xy_variation_Dense_sand	79.59	2.37	66.86	18.31	107	89	150	57
V2_3_impuls_0_6_vs_fracture_risk_horse_kick	15.00	0.11	4.52	3.05	20	4	10	9
V2_4_impuls_0_8_vs_fracture_risk_horse_kick	22.24	0.17	6.12	4.25	30	6	14	13
V2_5_impuls_1_0_vs_fracture_risk_horse_kick	27.89	0.21	7.69	5.45	37	8	17	17
V2_6_impuls_1_2_vs_fracture_risk_horse_kick	34.99	0.26	9.30	6.64	47	10	21	21
V2_7_impuls_1_4_vs_fracture_risk_horse_kick	41.39	0.31	10.80	7.82	56	12	24	24
V2_8_impuls_1_6_vs_fracture_risk_horse_kick	47.24	0.35	12.21	9.05	63	13	27	28
V2_9_impuls_1_8_vs_fracture_risk_horse_kick	52.03	0.41	13.66	10.40	70	15	31	32
V2_10_impuls_2_0_vs_fracture_risk_horse_kick	54.60	0.45	15.09	11.80	73	17	34	36
V2_11_impuls_2_2_vs_fracture_risk_horse_kick	55.92	0.48	16.66	13.27	75	18	37	41
V2_12_impuls_2_4_vs_fracture_risk_horse_kick	57.20	0.55	18.20	14.85	77	21	41	46
V2_13_impuls_2_6_vs_fracture_risk_horse_kick	58.34	0.86	19.97	16.55	78	32	45	51
V2_14_impuls_2_8_vs_fracture_risk_horse_kick	59.84	0.93	21.62	18.29	80	35	48	57
V2_15_impuls_3_0_vs_fracture_risk_horse_kick	61.48	1.16	23.33	20.02	82	44	52	62
V2_16_impuls_3_2_vs_fracture_risk_horse_kick	63.28	1.54	25.13	21.68	85	58	56	67
V2_17_impuls_3_4_vs_fracture_risk_horse_kick	64.57	1.72	26.77	23.26	87	65	60	72
V2_19_impuls_3_6_vs_fracture_risk_horse_kick	66.94	1.89	28.41	24.84	90	71	64	77
V2_20_impuls_3_8_vs_fracture_risk_horse_kick	68.72	2.57	29.99	26.43	92	96	67	82
V2_21_impuls_4_0_vs_fracture_risk_horse_kick	69.06	1.90	31.56	27.99	93	71	71	87
V2_14_Rotational_fall_Dense_sand	82.63	6.19	103.02	48.75	111	233	230	151

TABLE VII: AIS2+ INJURY RISK

The maximum predicted AIS2+ risk using shear stress (τ), maximum principle strain (ε), differential chest deflection (DcTHOR), and relative chest compression (Dmax) according to [2]. The last four columns provide results normalised with the trample simulation at the lower sternum location 6.

File Name [VEST_SimID_explaination]	τ AIS2+ %	ε_1 AIS2+ %	DcTHOR AIS2+ %	Dmax AIS2+ %	AIS2+ risk > 85% rib location. L=left. R=right.
V1_1_Trampled_angle_0_variation_stiff_ground	100	55	26	84	L4 R4
V1_2_Trampled_angle_20_variation_stiff_ground	1	23	100	84	-
V1_3_Trampled_angle_40_variation_stiff_ground	80	39	22	91	R6
V1_4_Trampled_angle_0H_variation_stiff_ground	78	87	1	74	L1 R1
V1_5_Trampled_angle_20H_variation_stiff_ground	20	82	30	61	R1
V1_6_Trampled_angle_40H_variation_stiff_ground	0	8	1	53	-
V1_7_Trampled_angle_0_variation_Soft_sand	40	18	0	15	-
V1_8_Trampled_angle_0_variation_Dense_sand	100	56	10	76	L4 R4
V1_9_Fall_angle_1xy_variation_Dense_sand	99	55	100	85	R4 R7
V1_10_Fall_angle_2x_variation_Dense_sand	100	82	100	85	L7 R1 R7 R8
V1_11_Fall_angle_3x_variation_Dense_sand	100	99	100	61	R1 R7 R8
V1_12_Fall_angle_2xy_variation_Dense_sand	100	100	100	43	R1 R2 R4 R6 R7 R8 R9
V1_13_Fall_angle_3xy_variation_Dense_sand	100	92	100	7	L1 R1 R4 R6 R7 R8
V1_3_impuls_0_6_vs_fracture_risk_horse_kick	0	0	0	0	-
V1_4_impuls_0_8_vs_fracture_risk_horse_kick	0	0	0	0	-
V1_5_impuls_1_0_vs_fracture_risk_horse_kick	0	0	0	2	-
V1_6_impuls_1_2_vs_fracture_risk_horse_kick	0	0	0	4	-
V1_7_impuls_1_4_vs_fracture_risk_horse_kick	0	1	0	6	-
V1_8_impuls_1_6_vs_fracture_risk_horse_kick	0	2	0	8	-
V1_9_impuls_1_8_vs_fracture_risk_horse_kick	1	5	0	13	-
V1_10_impuls_2_0_vs_fracture_risk_horse_kick	45	25	0	26	-
V1_11_impuls_2_2_vs_fracture_risk_horse_kick	99	35	0	39	L4 R4
V1_12_impuls_2_4_vs_fracture_risk_horse_kick	100	43	0	52	L4 R4
V1_13_impuls_2_6_vs_fracture_risk_horse_kick	100	48	0	64	L4 R4
V1_14_impuls_2_8_vs_fracture_risk_horse_kick	100	51	1	76	L4 R4
V1_15_impuls_3_0_vs_fracture_risk_horse_kick	100	55	2	84	L3 L4 R3 R4
V1_16_impuls_3_2_vs_fracture_risk_horse_kick	100	56	3	90	L3 L4 R3 R4
V1_17_impuls_3_4_vs_fracture_risk_horse_kick	100	57	5	92	L3 L4 R3 R4
V1_18_impuls_3_6_vs_fracture_risk_horse_kick	100	60	13	93	L3 L4 L5 R3 R4 R5
V1_19_impuls_3_8_vs_fracture_risk_horse_kick	100	61	25	94	L3 L4 L5 R3 R4 R5
V1_20_impuls_4-0_vs_fracture_risk_horse_kick	100	65	36	95	L3 L4 L5 R3 R4 R5
V1_14_Rotational_fall_Dense_sand	100	100	100	100	L1-9 R-9
V2_1_Trampled_angle_0_variation_stiff_ground	0	0	0	4	-
V2_2_Trampled_angle_20_variation_stiff_ground	0	0	0	5	-
V2_3_Trampled_angle_40_variation_stiff_ground	0	0	0	1	-
V2_4_Trampled_angle_0H_variation_stiff_ground	0	25	0	1	-
V2_5_Trampled_angle_20H_variation_stiff_ground	0	11	0	1	-
V2_6_Trampled_angle_40H_variation_stiff_ground	0	0	0	0	-
V2_7_Trampled_angle_0_variation_Soft_sand	0	0	0	0	-
V2_8_Trampled_angle_0_variation_Dense_sand	0	0	0	3	-
V2_9_Fall_angle_1xy_variation_Dense_sand	100	41	100	84	L1 L7 R1 R4 R7
V2_10_Fall_angle_2x_variation_Dense_sand	0	35	100	33	-
V2_11_Fall_angle_3x_variation_Dense_sand	100	98	100	18	11 R1 R7
V2_12_Fall_angle_2xy_variation_Dense_sand	100	63	0	6	R1 R6 R8
V2_13_Fall_angle_3xy_variation_Dense_sand	100	56	100	8	L1 R1 R8
V2_3_impuls_0_6_vs_fracture_risk_horse_kick	0	0	0	0	-
V2_4_impuls_0_8_vs_fracture_risk_horse_kick	0	0	0	0	-
V2_5_impuls_1_0_vs_fracture_risk_horse_kick	0	0	0	0	-
V2_6_impuls_1_2_vs_fracture_risk_horse_kick	0	0	0	0	-
V2_7_impuls_1_4_vs_fracture_risk_horse_kick	0	0	0	0	-
V2_8_impuls_1_6_vs_fracture_risk_horse_kick	0	0	0	0	-
V2_9_impuls_1_8_vs_fracture_risk_horse_kick	0	0	0	0	-
V2_10_impuls_2_0_vs_fracture_risk_horse_kick	0	0	0	2	-
V2_11_impuls_2_2_vs_fracture_risk_horse_kick	0	0	0	3	-
V2_12_impuls_2_4_vs_fracture_risk_horse_kick	0	0	0	5	-
V2_13_impuls_2_6_vs_fracture_risk_horse_kick	1	2	0	7	-
V2_14_impuls_2_8_vs_fracture_risk_horse_kick	1	3	0	8	-
V2_15_impuls_3_0_vs_fracture_risk_horse_kick	14	5	0	10	-
V2_16_impuls_3_2_vs_fracture_risk_horse_kick	34	7	0	21	-
V2_17_impuls_3_4_vs_fracture_risk_horse_kick	70	16	0	32	-
V2_19_impuls_3_6_vs_fracture_risk_horse_kick	99	14	0	42	L1 R1
V2_20_impuls_3_8_vs_fracture_risk_horse_kick	99	19	0	52	L1 R1
V2_21_impuls_4_0_vs_fracture_risk_horse_kick	100	28	1	62	L1 R1
V2_14_Rotational_fall_Dense_sand	100	100	100	100	L1-9 R-9